Environmental Science and Pollution Research (2020) 27:691–703
https://doi.org/10.1007/s11356-019-06904-2

RESEARCH ARTICLE

Effect of water leaching on biochar properties and its impact on organic contaminant sorption

Inga J. Schreiter[1] · Wolfgang Schmidt[2] · Abhay Kumar[3] · Ellen R. Graber[3] · Christoph Schüth[1]

Received: 14 June 2019 / Accepted: 28 October 2019 / Published online: 5 December 2019

Abstract

When biochar (BC) is applied to soil, one process that can alter its properties and contaminant sorption is the leaching of minerals and dissolved organic carbon (DOC). This study investigated changes in properties of three BCs (cattle manure, grain husk, and wood chips), due to leaching, and the subsequent impact on sorption of trichloroethylene (TCE) and tetrachloroethylene (PCE). The manure-derived BC released 27.4 mg g^{-1} DOC, which is over ten times more than that measured for the two plant-based BCs (2.5 and 1.5 mg g^{-1} DOC for grain husk and wood chips, respectively). In all leachates, potassium is the dominant cation, whereas chloride, sulfate, and phosphate are the main anions. In total, the manure-derived biochar released the highest sum of total ions (73.1 mg g^{-1}), followed by BC produced from grain husk (15.5 mg g^{-1}) and wood chips (1.2 mg g^{-1}). Leaching increased external surface area, mesopore volume, and hydrophobicity of the manure-derived BC and decreased its polarity. This enhanced sorption via partitioning. In plant-based BCs, micropore volume and size distribution were altered, most likely through the un-blocking of pores, causing increased sorption via pore-filling for both TCE and PCE. The results indicate that, depending on feedstock material, BC leaching can alter the environmental fate of organic compounds.

Keywords Biochar · Accelerated leaching · Leachable organic carbon · Pore clogging · Trichloroethylene · Tetrachloroethylene

Introduction

Sorbent materials prepared from biomass such as biochar (e.g., Zama et al. 2018) or activated carbon (e.g., Leite et al. 2018) are currently attracting increased attention in the scientific community. Biochar (BC) is a carbon-rich material produced via pyrolysis of organic material in an oxygen-limited atmosphere (Lehmann and Joseph 2009). In recent years, BC has sparked strong research interest due to its potential to confer a wide array of benefits when applied to soil (e.g., Xiao et al. 2018; Zhang et al. 2018). These include carbon sequestration (Lehmann and Joseph 2009), as well as agricultural benefits such as improved soil properties (Gul et al. 2015) and crop yield (Graber et al. 2010; Kumar et al. 2018). In addition, adding BC to soils of sites contaminated with inorganic and organic compounds can assist in their remediation (e.g., Kumar et al. 2016; Zhang et al. 2013).

When BC is used in remediation, the long-term effectiveness of sorption processes that reduce the mobility of contaminants is of prime interest (Ren et al. 2018). However, BC properties are affected by environmental exposure and interaction with the soil environment, which is summarized by the term "aging." Aging refers to several processes including leaching of minerals and organic carbon (OC) (Trigo et al. 2014), alteration of surface functional groups (Luo et al. 2017), and surface or pore blocking by organic matter (Kwon and Pignatello 2005) and minerals (Lin et al. 2012b). These mechanisms can significantly alter BC sorption behavior for organic contaminants. Reported effects of aging are

Responsible editor: Tito Roberto Cadaval Jr

Electronic supplementary material The online version of this article (https://doi.org/10.1007/s11356-019-06904-2) contains supplementary material, which is available to authorized users.

✉ Inga J. Schreiter
schreiter@geo.tu-darmstadt.de

[1] Institute of Applied Geosciences, Technische Universität Darmstadt, Schnittspahnstraße 9, 64287 Darmstadt, Germany

[2] Max-Planck-Institut für Kohlenforschung, Kaiser-Wilhelm-Platz 1, 45470 Mülheim an der Ruhr, Germany

[3] Department of Soil Chemistry, Plant Nutrition and Microbiology, Institute of Soil, Water and Environmental Sciences, Agricultural Research Organization, Volcani Center, P.O. Box 15159, 7505101 Rishon LeZion, Israel

diverse, ranging from increased sorption of herbicides (Trigo et al. 2014) to greatly attenuated sorption of nonionic organic compounds (Luo et al. 2017), and seem to depend on multiple factors like soil and initial BC characteristics, as well as compound properties.

Several studies have shown that leaching of minerals and OC from BC is one key process that occurs over the course of its aging. Studies examining leaching impact focus on nutrient release (Zhao et al. 2013), BCs' environmental fate and stability (Liu et al. 2018; Spokas et al. 2014), potential toxicity of BC-derived compounds (Smith et al. 2016), and the complexation between organic contaminants and released dissolved organic carbon (DOC) (Fu et al. 2018).

Two studies recently investigated the changes in sorption of organic compounds after removing leachable OC through washing. Wang et al. (2017) reported enhanced sorption of nitrobenzene, naphthalene, and atrazine by a rice straw BC, accelerated sorption kinetics, and reduced sorption irreversibility. This was mainly attributed to increased accessibility of micropores, due to the removal of leachable OC. Luo et al. (2017) also described enhanced sorption of nonionic organic compounds on two maize straw BCs after DOC removal, caused by exposure of initially blocked micropores. This suggests that the removal of DOC generally increases pore accessibility and therefore shows positive effects on contaminant immobilization. Further, Klasson et al. (2014) reported the unblocking of pores as a result of ash removal through rainwater washing. However, to the best of our knowledge, no study has been conducted investigating both DOC and mineral leaching, and linking the concomitant changes in the BC to its contaminant sorption ability.

Knowledge about the influence of initial BC properties on leaching and related processes is still limited, as most studies focused on only one BC type. In particular, the impact of BC leaching on its bulk properties and resulting changes in sorption mechanisms of organic contaminants have received only little attention. However, previous studies have shown that element (Wu et al. 2016) and DOC (Liu et al. 2019) leaching greatly differ with feedstock type and that structural properties and resulting sorption mechanisms are especially highly feedstock dependent (Schreiter et al. 2018).

Therefore, this study aims to link changes of BC properties due to leaching to changes that occur in contaminant sorption, by (i) investigating what is leached from BCs produced from different feedstocks, (ii) determining how leaching changes BCs' chemical and structural properties, and finally (iii) relating these changes to specific differences in sorption mechanisms. To achieve this, we artificially leached three BCs produced from cattle manure (BC-CM), grain husk (BC-GH), and wood chips (BC-WC), characterized the aqueous leachates, determined the changes in chemical and structural characteristics of the BCs, and analyzed their sorption behavior for two chlorinated compounds, trichloroethylene (TCE) and tetrachloroethylene (PCE).

Materials and methods

Biochar leaching

BCs were derived from cattle manure (BC-CM), grain husk (BC-GH), and wood ships (BC-WC) at a pyrolysis temperature of 450 °C. More details are available elsewhere (Schreiter et al. 2018). Methods for the leaching of soluble ions and OC described in the literature are diverse. Numerous studies utilize simple batch setups where BC is shaken with deionized water (e.g., Kloss et al. 2012; Spokas et al. 2014) or acidic solutions (e.g., de Figueredo et al. 2017; Klasson et al. 2014) at varying solid to liquid ratios and shaking times. However, also repeated washing cycles (e.g., Angst and Sohi 2013; Luo et al. 2017), continuous in-column leaching (Feng et al. 2018), and the simulation of weathering in a Soxhlet extractor (Yao et al. 2010) have been reported. As several studies suggest that leaching kinetics can be slow (Angst and Sohi 2013; Kong et al. 2014), we chose an accelerated leaching method utilizing an accelerated solvent extractor. A similar method was previously used to extract pyrogenic water-soluble organic matter from biochars (Norwood et al. 2013). The elevated pressure and temperature applied in accelerated solvent extraction should allow rapid and complete mobilization of soluble compounds. Therefore, application of this method should yield the maximum amount of leachable compounds.

Accelerated leaching was performed with an accelerated solvent extractor (ASE 300, Dionex, Germany). Stainless steel extraction cells (33 mL) were filled with 1.5 g of BC and glass fiber filters (Thermo Scientific, Germany) at the top and bottom of the extraction cell. All BCs were extracted with deionized water (ultra-pure Millipore) at 100 °C for 10 min under 100 bar cell pressure (more details in the Supplementary Material). Aqueous extracts were collected in 200-mL glass bottles fitted with screw caps and rubber septa. Each extraction was performed with three replicates, each yielding about 60 to 65 mL of leachate. After the extracts were cooled to room temperature, electrical conductivity (EC) and pH were measured (PCE-PHD1, PCE Instruments, Germany). All leachates were stored refrigerated until further analysis. Leached BC samples were dried for 24 h at 105 °C and stored in amber glass bottles until further use.

Characterization of aqueous leachates

All leachates were filtered using 0.45-μm cellulose acetate filters. Dissolved organic carbon (DOC) was determined with a carbon analyzer equipped with an IR detector (LiquiTOC II, Elementar, Germany). Major cations (sodium (Na^+), potassium (K^+), magnesium (Mg^{2+}), calcium (Ca^{2+}), ammonium (NH_4^+)) and anions (fluoride (F^-), chloride (Cl^-), bromide (Br^-), nitrite (NO_2^-), nitrate (NO_3^-), phosphate (PO_4^{3-}),

sulfate (SO_4^{2-})) were determined by ion chromatography (882 Compact IC plus, Metrohm, Switzerland).

Characterization of original and leached biochars

For the characterization of the leached BCs, triplicate samples were combined and thoroughly mixed. All samples were characterized with methods as described in Schreiter et al. (2018). In brief, the bulk elemental composition (C, H, N, and S) was determined with an elemental analyzer (vario EL cube, Elementar, Germany; performed by Zeta Partikelanalytik, Mainz, Germany), organic carbon content (C_{org}) using a carbon analyzer with IR detector (LiquiTOC II, Elementar, Germany), and ash content gravimetrically after heating the samples to 750 °C for 6 h (ASTM D 1762-84 2013). The oxygen (O) content was determined by difference (Kah et al. 2016). Bulk elemental analysis was conducted in duplicates, C_{org}, and ash content in triplicates. Molar ratios describing aromaticity (H/C), hydrophobicity (O/C), and polarity ((O + N)/C) were calculated from bulk elemental composition. Specific surface area (SSA), external surface area (SSA_{ext}), total pore volume (PV_{tot}), micropore volume (PV_{mic}), and pore size distribution were analyzed by argon sorption (at 87 K) using a Micromeritics 3Flex sorption analyzer (more details in Schreiter et al. 2018).

For the analysis of mineral elements, original and leached BCs were ashed at 1000 °C for 1 h. The residue was then fused with lithium metaborate at 1000 °C, dissolved in 100 mL acid (4% HNO_3/2% HCl), and analyzed by inductively coupled plasma–atomic emission spectroscopy (ICP-AES). Results are reported as mass of element per mass bulk sample (all analysis performed by ALS Minerals, Loughrea, Ireland).

Batch sorption experiments

Sorption experiments with trichloroethylene (TCE) and tetrachloroethylene (PCE) were carried out as previously described (Schreiter et al. 2018). In brief, experiments were performed in headspace vials with 50 mL of 0.01 M Na_2ClO_4 as a background solution. For each compound, three initial concentrations were prepared (TCE 1.7 mg L^{-1}, 22 mg L^{-1}, 110 mg L^{-1}; PCE 1.9 mg L^{-1}, 19.8 mg L^{-1}, 108 mg L^{-1}). To each vial, an appropriate amount of BC (between 1.5 mg and 0.45 g) was added to achieve a 20 to 90% reduction in solute concentration after sorption. The compound of interest was spiked dissolved in methanol (between 20 and 125 μL). Triplicate samples were agitated on a horizontal shaker for 7 days under ambient conditions (21 °C ± 1) to reach apparent equilibrium as determined in preliminary experiments (data not shown), accompanied by blank and sorbent-free control samples. After 7 days, aqueous phase concentrations were determined by static headspace sampling, gas chromatographic separation, and flame ionization (FID) or electron capture (ECD) detection (more details in Schreiter et al. 2018).

Data analysis

Most sorption studies utilize the Freundlich isotherm model to evaluate their data. However, Carmo et al. (2000) have raised concern about the use of the Freundlich coefficient, especially for the comparison of sorbates with different aqueous solubilities, because of its concentration dependent nature. Therefore, the unit-equivalent Freundlich model was used for data evaluation in this study as also applied by others (Allen-King et al. 2002; Carmo et al. 2000; Kleineidam et al. 2002):

$$C_S = K_{Fr}{}^*(C_W/S_W)^{\mathrm{n}} \quad (1)$$

where S_W (mg L^{-1}) is the water solubility of the compound, C_W (mg L^{-1}) the aqueous concentration at equilibrium, and C_S (mg kg^{-1}) the sorbed concentration on the solid phase, calculated by mass balance. K_{Fr}* (mg kg^{-1}) and n (–) are the unit-equivalent Freundlich coefficient and Freundlich exponent, respectively.

Multiple studies reported that pore-filling is one important mechanism in organic contaminant sorption on BCs (e.g., Nguyen et al. 2007). It can be described by Polanyi's potential theory and is represented in the Polanyi-Dubinin-Manes isotherm model (Allen-King et al. 2002). As BC is a highly heterogeneous material, additional mechanisms might contribute to sorption. Several researchers reported that it can follow a combined pore-filling and partitioning process (e.g., Chen et al. 2008). This can be expressed in a combined isotherm model as proposed by Xia and Ball (1999). It combines linear partitioning with a Polanyi theory–based pore-filling term:

$$C_S = V_0\,\rho \exp\left[-\left[\frac{RT\left(-\ln\frac{C_W}{S_W}\right)}{E}\right]\right]^b + K_p C_W \quad (2)$$

where S_W (mg L^{-1}) is the water solubility of the compound, C_W (mg L^{-1}) the aqueous concentration at equilibrium, C_S (mg g^{-1}) the adsorbed concentration, V_0 (cm^3 kg^{-1}) the maximum adsorbed volume of sorbate per unit mass, K_p (L kg^{-1}) the linear partitioning coefficient, ρ (g cm^{-3}) the sorbate density, E (J mol^{-1}) the characteristic free energy of adsorption, R (J (mol*K) $^{-1}$) the ideal gas constant, and T (K) the absolute temperature. To minimize the number of fitting parameters, b (–) is fixed to $b = 2$ (Dubinin-Radushkevich equation).

Statistical analysis

The data of leached compounds (ions and DOC) and the BC properties were analyzed by one-way analysis of variance (ANOVA) with Tukey's post-hoc test to determine significant differences (SigmaPlot 12.0, Sysstat Software Inc., USA). Results of $p > 0.05$ are considered not significant.

Sorption coefficients including standard errors and confidence intervals were derived by dynamic curve fitting in the software SigmaPlot 12.0 (Sysstat Software Inc., USA). For both isotherm models, sorption coefficients of different data sets were considered to be significantly different when their 95% confidence intervals did not overlap ($p < 0.01$) or did not overlap by more than 50% ($p < 0.05$) (Cumming 2009).

Results and discussion

Leaching of extractable ions and change in mineral content

Table 1 and Table S3 summarize the characteristics of the aqueous leachates of the three BCs. All leachates are alkaline and pH values are similar to those determined for the original bulk BCs (Tables 1 and 2). The BC-CM extract shows the highest and BC-GH the lowest pH value (10.2 and 8.3, respectively). BC-CM leachate exhibits the highest EC, followed by BC-GH and BC-WC (3757, 643, and 147 μS cm^{-1}, respectively; all statistically different; $p < 0.01$). EC tends to increase with increasing ash content of the original BCs. However, there is no significant linear correlation, because the ash composition varies and only selected minerals dissolve and contribute to the leachate EC. A similar trend as described for EC is present for the total amount of leached ions. BC-CM released the highest sum of total ions (73.1 mg g^{-1}), followed by BC-GH (15.5 mg g^{-1}) and BC-WC (1.2 mg g^{-1}) (all significantly different with each other; $p < 0.01$). K^+ and Na^+ are the dominating cations in the leachates of all three BCs. The leaching of Ca^{2+} and Mg^{2+} is comparatively low, which is similar to results reported in other studies (Kong et al. 2014; Yao et al. 2010). The anions with the highest concentrations in all leachates are Cl^-, SO_4^{2-}, and PO_4^{3-}. However, the proportions vary depending on the leached BC. Cl^- dominates the BC-CM leachate, whereas the leachates of BC-WC and BC-GH are characterized by high SO_4^{2-} and PO_4^{3-} concentrations, respectively. The leaching of N-species from all three BCs (in the form of NO_3^-, NO_2^-, and NH_4^+) is comparatively low, as also found by others (Graber et al. 2010), because they are likely bound in sparsely soluble form (Hollister et al. 2013).

Table 1 Selected characteristics of aqueous leachates of the three biochars (BCs). Dissolved organic carbon (DOC) and ion content leached were calculated from the concentration (mg L^{-1}) measured in the leachate, mass of BC leached (g), and volume of leachate (mL). Note the differing units for Ca^{2+} and Mg^{2+}

	BC-CM	BC-GH	BC-WC
pH (-)	10.2 ± 0.04	8.3 ± 0.03	8.8 ± 0.05
EC (μS cm^{-1})[a]	3,757 ± 78	599 ± 7	147 ± 4
DOC (mg g^{-1})	27.4 ± 0.4	2.5 ± 0.1	1.5 ± 0.1
K^+ (mg g^{-1})	31.8 ± 0.5	7.5 ± 0.1	0.6 ± 0.02
Na^+ (mg g^{-1})	10.0 ± 0.1	0.3 ± 0.03	0.2 ± 0.01
Ca^{2+} (μg g^{-1})	435 ± 94	92 ± 6	73 ± 4
Mg^{2+} (μg g^{-1})	66 ± 16	57 ± 4	28 ± 1
PO_4^{3-} (mg g^{-1})	1.5 ± 0.1	5.3 ± 0.1	0.1 ± 0.001
SO_4^{2-} (mg g^{-1})	4.5 ± 0.1	1.1 ± 0.02	0.2 ± 0.004
Cl^- (mg g^{-1})	24.2 ± 0.4	1.0 ± 0.05	0.1 ± 0.01
Total ions leached (mg g^{-1})[b]	73.1 ± 1.0	15.5 ± 0.1	1.2 ± 0.03

[a] EC: electrical conductivity of the leachate

[b] Sum of all ions measured with ion chromatography. For all measured ions, refer to Table S3

The ion concentrations detected in the leachates are in line with the changes determined for the content of respective mineral elements in the bulk of BCs before and after leaching (Table S4). Ca and Mg tend to accumulate in the bulk sample or show only small changes. Na, K, and P contents in BC-CM and BC-GH decrease notably. In BC-WC, Na tends to accumulate and changes in K and P are negligible.

According to Wu et al. (2011) the leaching of inorganic species predominantly depends on their initial form of occurrence in BC. Most leached ions originate from the dissolution of mineral components in the ash fraction of the BCs. Ca and Mg are often bound in hardly soluble carbonates or carboxylates (Wu et al. 2011), explaining their comparably low concentrations in all BC leachates and accumulation in the bulk samples. The Cl^- concentrations show a positive significant ($p < 0.05$) correlation with K^+ and Na^+ in all leachates, suggesting the dissolution of halite (NaCl) and sylvite (KCl). In BC-CM leachates, the mean K^+/Cl^- molar ratio of 1.19 ± 0.01 (Table S5) suggests that sylvite dissolution is the main K^+ source. Sylvite is one of the most common minerals in BC (Xu et al. 2017), and several studies identified sylvite in BCs produced from various feedstocks, including dairy manure (Cao and Harris 2010), straw (Kloss et al. 2012), and plant material (Zhao et al. 2013). For the plant-based BCs (BC-WC and BC-GH), a K^+ excess over Cl^- is present (K^+/Cl^- molar ratios >> 1; Table S5), suggesting the additional contribution of other soluble minerals such as phosphates, sulfates, or carbonates. Xu et al. (2017) reported that K-bearing minerals are typical for crop-residue BC. The molar ratios of (Na + K + 2Mg + 2Ca)/(Cl + 2S + 3P) in the leachates of BC-WC (3.22 ± 0.09), and BC-CM (1.55 ± 0.02) clearly exceed unity (Table S5). This suggests that in addition to soluble salts, some of the released cations exist in other water-soluble forms in BCs, such as Na^+ and K^+ ion-exchangeable carboxylates (Wu et al. 2011). In contrast, the molar ratio in the leachate of BC-GH (0.98 ± 0.01; Table S5) indicates no major contribution of leaching from carboxylates.

As the leachates varied depending on the BC, it is evident that their composition greatly depends on the binding form, the ash composition, and the associated release mechanism of the different ions. These in turn are determined by the original feedstock composition and pyrolysis conditions. The

Table 2 Properties of the original and leached biochars (BCs)

	BC-CM		BC-GH		BC-WC	
	Original[a]	Leached	Original[a]	Leached	Original[a]	Leached
EC (μS cm^{-1})[b]	7,910	834	764	281	242	133
pH (−)[b]	10.3	9.5	8.3	7.9	9.8	7.8
C (%)	22.7	25.2	55.8	56.7	73.7	74.7
H (%)	1.1	1.6	3.3	3.1	2.5	2.6
N (%)	1.3	1.3	1.5	1.5	0.5	0.5
S (%)	0.7	0.5	0.4	0.5	0.4	0.2
Ash content (%)	62.8	61.9	26.6	25.1	12.5	9.5
C_{org} (%)	23.5	22.9	53.7	52.9	68.7	70.6
O (%)[c]	11.4	9.5	12.4	13.0	10.5	12.8
H/C[d]	0.55	0.76	0.71	0.65	0.40	0.41
O/C[d]	0.38	0.28	0.17	0.17	0.11	0.13
(O + N)/C[d]	0.43	0.33	0.19	0.19	0.11	0.14
SSA (m^2 g^{-1})[e]	6	25	215	214	341	342
SSA_{ext} (m^2 g^{-1})[f]	6	25	60	46	58	36
PV_{tot} (cm^3 g^{-1})[g]	0.023	0.046	0.136	0.124	0.173	0.157
PV_{mic} (cm^3 g^{-1})[h]	n.d. [k]	n.d. [k]	0.061	0.064	0.109	0.116
PV_{mes} (cm^3 g^{-1})[i]	0.023	0.046	0.075	0.060	0.064	0.041
D_{mic} (nm)[j]	n.d. [k]	n.d. [k]	0.78	0.78	0.64	0.79
D_{mes} (nm)[j]	n.d. [k]	n.d. [k]	2.9	2.9	2.8	2.9

[a] Data obtained from Schreiter et al. (2018)

[b] Electrical conductivity (EC) and pH determined in a 1:10 BC to water suspension

[c] O determined by difference

[d] Molar ratios describing aromaticity (H/C), hydrophobicity (O/C), and polarity ((O + N)/C) of BCs (ratios based on bulk elemental composition)

[e] Apparent specific surface area (BET method)

[f] Specific external surface area (t-plot method)

[g] Total pore volume determined at $P/P_0 = 0.995$

[h] Micropore volume (t-plot method)

[i] Mesopore volume ($PV_{tot} - PV_{mic}$)

[j] Maxima of micropore and mesopore distribution (NLDFT method)

[k] Not determined

concentrations determined in our study are within the range of values reported in the literature (Table S6). However, one should be cautious in comparing reported results, as leaching protocols are diverse and vary greatly in extraction time, extraction temperature, and BC to water ratio.

Leaching of dissolved organic carbon

The leaching procedure mobilized DOC from all BCs (Table 1). The manure-derived BC-CM released the highest amount of DOC (27.4 mg g^{-1}), which is about 10 times more than determined for the two plant-based BCs. BC-GH and BC-WC leached 2.45 mg g^{-1} and 1.53 mg g^{-1}, respectively (all statistically different; $p < 0.01$). The leached DOC tends to increase with increasing O/C and (O + N)/C ratio of the original BC, although both correlations are not statistically significant ($p > 0.05$). However, it suggests that BCs with high polarity and low hydrophobicity can mobilize more DOC. Liu et al. (2019) found that DOC release is positively correlated with the O and H contents of BC, as well as with its aromaticity ratio (H/C ratio). They concluded that the DOC was mainly released from biochars' labile fraction that is rich in oxygen-containing functional groups (Liu et al. 2019). Although our data do not show these correlations, the trends observed for O/C and (O + N)/C ratios indicate the importance of functional groups in DOC release, as especially (O + N)/C is a good proxy for oxygen functionalities (Chen et al. 2008). The wood-based BC-WC released substantially lower DOC concentrations than BC-GH and BC-CM. This is in line with the findings by Liu et al. (2019) that BC produced from wood generally releases less DOC than BCs from herbaceous or manure feedstock. Wood contains more lignin, which is

thermally more stable than cellulose and hemicellulose (Yang et al. 2007), and therefore tends to produce BC with less leachable bio-oil components (Liu et al. 2019).

The DOC concentrations determined in our study are in a similar range as previously reported by Norwood et al. (2013). They examined ASE extraction of cordgrass and honey mesquite BCs and reported concentrations of 21.5 mg g^{-1} and 16.0 mg g^{-1}, respectively. In general, our findings are in line with previous studies that DOC release differs for different BCs (e.g., Liu et al. 2019; Qu et al. 2016; Smith et al. 2016), indicating that it depends on the BC feedstock material. However, Liu et al. (2019) also state that pyrolysis temperature is a more important factor in DOC development than feedstock material.

Change of biochar bulk properties after leaching

A summary of the BC bulk properties before (obtained from Schreiter et al. 2018) and after leaching is presented in Table 2. The C content of all BCs tends to increase after leaching; however, only the change in BC-CM is significant ($p < 0.05$). Simultaneously, the wood-based BC-WC shows a significant increase in C_{org} ($p < 0.05$), whereas the changes in BC-CM and BC-GH are not significant ($p > 0.05$). Several studies reported increasing C content after varying leaching protocols (Luo et al. 2017; Qu et al. 2016; Spokas et al. 2014; Wang et al. 2017); however, decreasing C content after weathering or leaching was also reported (Christophe et al. 2015). The different development in C and C_{org} content is likely a result of the relative distribution of inorganic species and mobile organic matter in the different BCs. The increase of C_{org} in BC-WC is in line with the relatively small amount of DOC leached and the assumption that lignin forms more stable carbon structures during pyrolysis (Yang et al. 2007). In contrast, C_{org} of BC-GH and BC-CM tends to decrease after leaching because of their higher DOC loss caused by more labile carbon formed through the pyrolysis of cellulose and hemicellulose (Yang et al. 2007). One possible reason for the increase in total C content is the effect of the low leachability of carbonates (Wu et al. 2011) as discussed earlier. This can result in the enrichment of relatively stable inorganic carbon phases compared to easily soluble labile OC and other mineral components. In line with this argument is the decrease of EC and ash content of all BCs after leaching ($p < 0.01$), as also reported in other studies (Wu et al. 2011). Additionally, all BCs exhibit decreasing pH values, which can be explained by the release of alkaline base cations (Table 1) during leaching (Yao et al. 2010).

Both plant-based BCs (BC-GH and BC-WC) show a slight increase of O in the bulk mass. In contrast, the O content in BC-CM decreases after leaching (Table 2). This is accompanied by increasing hydrophobicity (decreasing O/C ratio) and decreasing polarity (decreasing (O + N)/C ratio) of BC-CM. As the polarity ratio is a good indicator for oxygen-bearing functional groups (Chen et al. 2008), decreasing (O + N)/C and subsequent decreasing O content indicate the loss of polar functionalities during DOC leaching. Qu et al. (2016) found that the O/C ratio of released DOC was twice as high as the O/C ratio of the bulk BC, confirming that polar functional groups are lost during the leaching process. This also results in less clustering of water molecules on the BC surface (Chun et al. 2004), making the surface more hydrophobic. The two plant-based BCs show no relevant change in O/C and (O + N)/C ratios, which is in agreement with their significantly lower DOC leaching.

Change of biochar surface and pore structure after leaching

Figure 1 shows the incremental pore size distribution and the cumulative pore volume of the three BCs before and after leaching. The calculated SSA, SSA_{ext}, PV_{tot}, and PV_{mic} are listed in Table 2. The changes in SSA of BC-WC and BC-GH are negligible. However, leaching of BC-WC notably changed the pore size distribution, especially in the range smaller than 2 nm. The maximum of the micropore distribution (D_{mic}) shifted towards bigger pores, now being 0.79 nm instead of 0.64 nm, and the determined PV_{mic} slightly increased compared to original BC-WC. Figure 1 illustrates that additional pore volume developed in the range of 0.5 to 2 nm.

The other plant-based char, BC-GH, shows only small changes. The pore size distribution of leached BC-GH displays a slightly higher fraction of pores around 1.2 nm pore width (Fig. 1), whereas pores between 0.8 and 1 nm pores disappeared. Consequently, only marginal changes of PV_{mic} are detected. A reason could be the collapse of pore walls during leaching. Spokas et al. (2014) identified cracks, fractures, and "sinkhole-like" features after 24 h rinsing of different BCs. This might also be the cause for lower SSA_{ext}, PV_{mes}, and PV_{tot} in both plant-based BCs.

The manure-derived BC-CM shows distinctly different behavior. Both original and leached BC-CM contain their entire SSA in mesopores, captured in SSA_{ext}. It is more than 4 times higher in the leached sample than determined in the original BC-CM. Consequently, PV_{mes} doubled through the development of additional pore volume mainly in the range of 2 to 10 nm pore width. Although PV_{tot} increased, no micropores are present in leached BC-CM, as well as in the original sample.

The described changes in the pore size distribution, pore volume, and SSA of the different BCs illustrate that leaching significantly affects their structural properties. However, the impact of leaching varies between the BC types.

Although BC-WC released only a small amount of mineral components (1.2 mg g^{-1} ions) and DOC (1.5 mg g^{-1}), the effect on the micropore size distribution and pore volume is significant. In contrast, the leaching of BC-GH has only minor

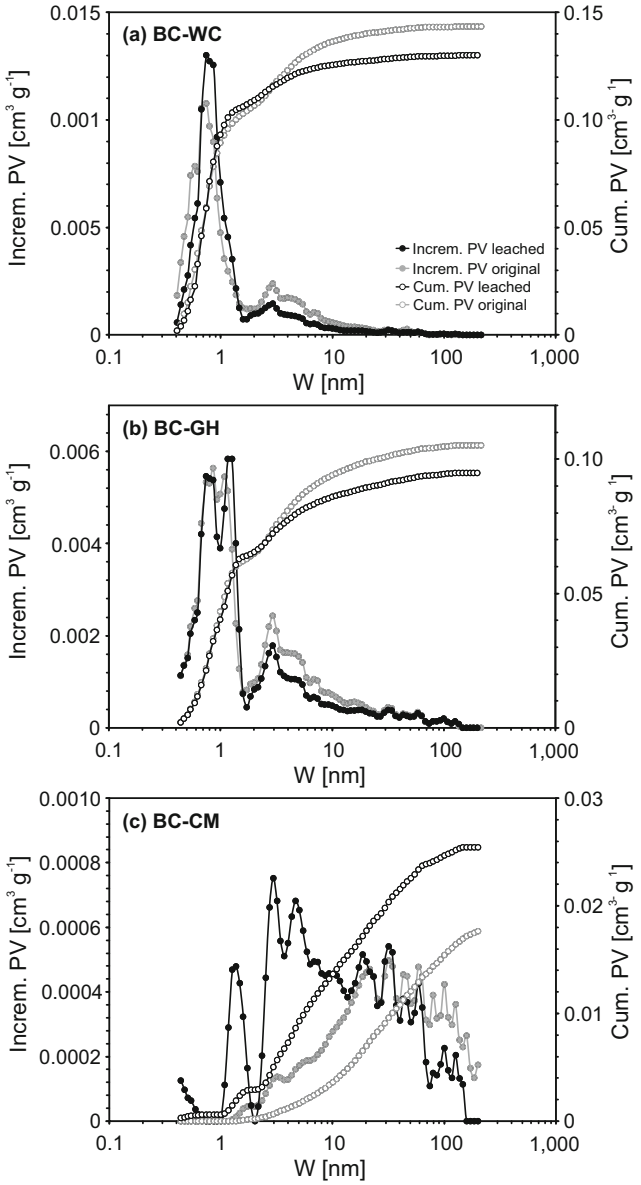

Fig. 1 Incremental pore size distribution (Increm. PV ($cm^3\ g^{-1}$); filled symbols) and cumulative pore volume (Cum. PV ($cm^3\ g^{-1}$); open symbols) of the three biochars (**a** BC-WC, **b** BC-GH, **c** BC-CM) before (gray) and after (black) leaching. Data was obtained by argon sorption and analyzed using a non-local density function theory (NLDFT) assuming argon sorption in slit-shaped pores. W (nm) corresponds to the pore width. Data for original BCs (gray) were previously published in a similar form in Schreiter et al. (2018)

impact on its structural properties, despite the higher concentrations of ions (15.5 mg g^{-1}) and DOC (2.45 mg g^{-1}) released. In BC-CM, leaching of comparatively high amounts of mineral species (73.1 mg g^{-1}) and DOC (27.42 mg g^{-1}) resulted in no change in small pores but extensive alterations in the mesoporous range and SSA. This indicates that leaching does not affect all BCs equally. Depending on the initial distribution and binding of ions and DOC, the response to leaching is different.

Previous studies (Luo et al. 2017; Wang et al. 2017) have shown that DOC can be trapped in small pores and act as a pore-clogging agent. Therefore, leaching generally increased pore accessibility. Luo et al. (2017) reported that the removal of authigenic DOC from two maize straw BCs caused a slight increase in the total surface area (SA) by exposing initially blocked micropores. Wang et al. (2017) stated that the change in SA after DOC leaching was negligible in a rice straw BC, but total and micropore volume significantly increased. Both plant-based BCs in our study show increasing PV_{mic} after leaching, which can be linked to the unblocking of micropores through DOC release. However, the effect is more pronounced in BC-WC compared to BC-GH. This indicates that the pore-clogging effect might be more important if a high number of small micropores are already available in the original BC. Indeed, Luo et al. (2017) suggested that pore blockage may play a bigger role in BCs with higher SA and porosity. Further, several researchers found that the nature and composition of the leached DOC can vary greatly for different BCs (e.g., Jamieson et al. 2014; Lin et al. 2012a; Smith et al. 2013; Tang et al. 2016). Therefore, DOC in BCs derived from different feedstocks might exhibit different binding characteristics, including pore filling and pore blocking. This would result in varying release mechanisms depending on DOC properties and composition.

Similar to DOC, the release of mineral components can also alter the pore structure of BCs. Klasson et al. (2014) showed that washing of several microporous BCs produced from almond shell, removed ash, and exposed SA as well as some previously blocked small pores. Thereby, the pore structure was more affected in low-ash BCs (Klasson et al. 2014). Further, Spokas et al. (2014) confirmed that salts can be precipitated in BC pores and limit their availability. This indicates that the change in PV_{mic} and the micropore distribution might, at least partly, be caused by the release of soluble ions.

Despite being released from pores, DOC can also be mobilized via the surface functional groups, which does not affect the structural properties. This is likely the case for BC-CM, as its decreasing (O + N)/C ratio indicates the loss of surface functionalities via DOC leaching. Additionally, structural changes of BC-CM are controlled by the leaching of mineral components or DOC from larger pores and the outer BC surface. This explains the substantial increase of SSA_{ext} and PV_{mes}. Spokas et al. (2014) confirmed with SEM-EDS studies that surface precipitates and organic oils coated surfaces and concealed visible pores in fresh BCs. The removal of these precipitates and surface coatings via dissolution opened additional porosity and exposed new structural details (Spokas et al. 2014).

However, to distinguish between DOC and mineral release-driven structural changes in BC is challenging, as the spatial arrangement and distribution of mineral and organic phases are feedstock dependent (Yang et al. 2018). Both phases are usually interlaced and interact with each other (Xiao et al. 2018). Yet,

our results suggest that the unclogging of micropores is mainly related to DOC leaching, whereas the exposing of mesopores and SSA_{ext} is caused by mineral leaching.

Sorption to leached biochars

To assess the effect of the leaching and resulting changes in BC properties, equilibrium batch experiments were conducted, with original (Schreiter et al. 2018) and leached BCs. The unit-equivalent Freundlich model (Eq. 1) was fitted to all sorption data, and the results are presented in Fig. S2 and Table 3.

As previously described (Schreiter et al. 2018), sorption affinity K_{Fr}* of both TCE and PCE increases following BC-CM < BC-GH < BC-WC. The same pattern is still observed after BCs are leached, although sorption of both compounds tends to increase after leaching ($K_{Fr}*_{orig.} < K_{Fr}*_{leach.}$). PCE sorption to all three BCs is significantly enhanced after leaching ($p < 0.01$). With an increase of 19%, BC-CM exhibits the strongest change, followed by BC-WC (18%) and BC-GH (17%). Considering TCE sorption, only BC-CM shows a significant increase ($p < 0.01$) in K_{Fr}* (26%), whereas the changes in sorption to BC-GH and BC-WC are not significant. This illustrates that the changes in sorption affinity differ distinctly not only between compounds but also between BCs. For both compounds, the increase in K_{Fr}* is highest for the manure-derived BC-CM that also released the most DOC and leachable ions. However, the increasing sorption of PCE to the plant-derived chars BC-WC and BC-GH cannot be immediately explained by the amount of leachable minerals and OC, as it is comparatively small.

The sorption nonlinearity is much less affected by the leaching procedure. Only BC-CM shows significant changes, with slightly increasing n for both TCE (original 0.39; leached 0.43; $p < 0.05$) and PCE (original 0.46; leached 0.52; $p = 0.05$). This suggests increased linear sorption, which in turn indicates stronger partitioning of both sorbates. As previously discussed, BC-CM is the only sorbent with significantly lower polarity and higher hydrophobicity after leaching. This reduces the adsorption of water molecules (Chun et al. 2004; Li et al. 2002) and therefore might increase the accessibility of the BC matrix for partitioning.

Change in sorption mechanisms after biochar leaching

Sorption of organic contaminant to BC usually comprises multiple mechanisms (e.g., Xiao et al. 2018), in which pore-filling and partitioning dominate in case of chlorinated hydrocarbons (Schreiter et al. 2018). These processes are influenced by the compound properties, e.g., the water solubility and molecular size of the sorbate, but also BC characteristics. The Polanyi theory–based adsorption-partitioning model (Eq. 2) allows to resolve the contribution of partitioning and pore-filling to the overall sorption and should help to further explore the changes in sorption mechanisms after leaching. The respective isotherms are displayed in Fig. 2, and fitting parameters are reported in Table 4.

Sorption of TCE to both plant-based BCs (BC-WC and BC-GH) after leaching is well described by a sole pore-filling mechanism (K_p derived from the model fit not significant; $p > 0.01$). The partitioning component that contributed to TCE sorption to the original BC-GH (Schreiter et al. 2018) is eliminated entirely after leaching (Table S7). In contrast, the manure-derived BC-CM shows significant influence of partitioning for the sorption of both compounds, as do the isotherms of PCE sorption to BC-GH and BC-WC, before and after leaching.

Table 3 Parameters of the unit-equivalent Freundlich model for trichloroethylene (TCE) and tetrachloroethylene (PCE) sorption to original and leached biochars (BCs)

			K_{Fr}* (mg kg^{-1})[b]	n (–)[b]	r^2 (–)[c]	p (–)[c]
TCE	BC-WC	Original[a]	209,143 ± 12,730	0.26 ± 0.02	0.96	< 0.01
		Leached	228,452 ± 12,813	0.26 ± 0.01	0.97	< 0.01
	BC-GH	Original[a]	140,467 ± 6,176	0.32 ± 0.01	0.99	< 0.01
		Leached	141,489 ± 6,511	0.30 ± 0.01	0.98	< 0.01
	BC-CM	Original[a]	29,503 ± 806	0.39 ± 0.01	0.99	< 0.01
		Leached	39,828 ± 1,496	0.43 ± 0.01	0.99	< 0.01
PCE	BC-WC	Original[a]	108,260 ± 3,345	0.33 ± 0.02	0.97	< 0.01
		Leached	132,431 ± 4,695	0.30 ± 0.02	0.96	< 0.01
	BC-GH	Original[a]	74,484 ± 2,974	0.33 ± 0.02	0.97	< 0.01
		Leached	90,228 ± 2,937	0.33 ± 0.01	0.98	< 0.01
	BC-CM	Original[a]	14,802 ± 365	0.46 ± 0.02	0.99	< 0.01
		Leached	18,375 ± 435	0.52 ± 0.02	0.99	< 0.01

[a] Recalculated from data published in Schreiter et al. (2018).

[b] Unit -equivalent Freundlich coefficients K_{Fr}* and Freundlich exponents n calculated using non-linear curve fitting in Sigma Plot after Eq. 1

[c] r^2 and p represent the coefficient of determination and significance of the data fit obtained from Sigma Plot

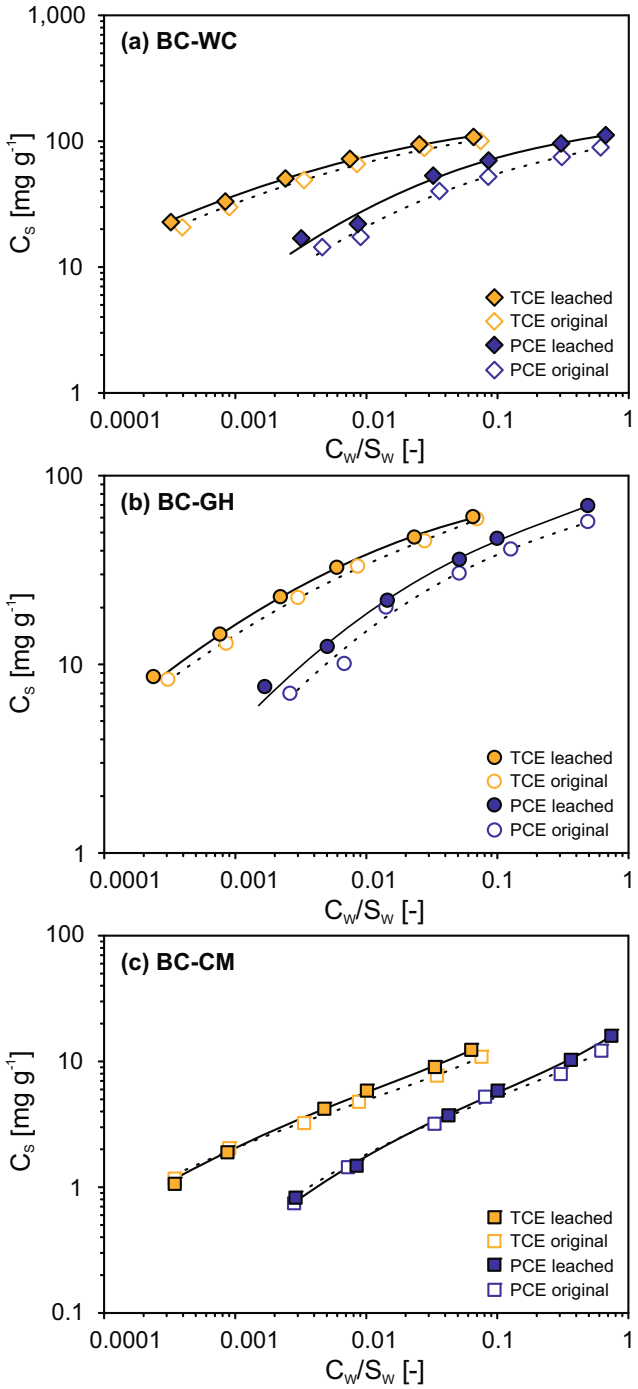

Fig. 2 Sorption isotherms of trichloroethylene (TCE) and tetrachloroethylene (PCE) to the three biochars (**a** BC-WC, **b** BC-GH, **c** BC-CM) before (open symbols) and after (filled symbols) leaching. Dashed (before leaching) and solid (after leaching) lines represent the fitted Polanyi-based adsorption-partitioning model (Eq. 2). All data points represent the average of triplicate data. All error bars are within symbol size. Data for sorption to original BCs (open symbols) were previously published in Schreiter et al. (2018)

For all three leached BCs, the maximum adsorbed volume V_0 is significantly higher for TCE compared to PCE ($V_0{}^{TCE}{}_{leach.} > V_0{}^{PCE}{}_{leach.}$; $p < 0.01$), displaying the same trend as observed in the original BCs (Schreiter et al. 2018). V_0 for TCE increases significantly after leaching for BC-WC and BC-GH, with 7.5% and 15.7% respectively (both $p < 0.01$). The V_0 value of BC-CM also increases (about 21%; $p < 0.05$) but is still about one order of magnitude lower than V_0 of the two other leached BCs. Considering PCE, only V_0 of BC-WC shows a significant increase (27%; $p < 0.01$), whereas the changes for BC-GH (12.4%) and BC-CM (5%) are not significant ($p > 0.05$).

As discussed earlier, Fig. 1 shows that BC-WC experienced significant changes in its micropore size distribution. Leaching created additional pore volume in the region between 0.5 nm and 2 nm, which is reflected in its increased PV_{mic}. The availability of additional micropores and the concomitant shift towards slightly larger pore sizes allows PCE and TCE to penetrate a larger number of sorption sites in leached BC-WC. This is reflected in higher V_0 of both compounds after leaching ($V_0{}^{TCE}{}_{leach.} > V_0{}^{TCE}{}_{orig.}$; $V_0{}^{PCE}{}_{leach.} > V_0{}^{PCE}{}_{orig.}$; both $p < 0.01$). However, TCE is still able to access a larger number of pores ($V_0{}^{TCE}{}_{leach.} > V_0{}^{PCE}{}_{leach.}$; $p < 0.01$). This is the result of a steric effect caused by molecular sieving, as already observed in the original BC-WC (Schreiter et al. 2018). TCE is the slightly smaller molecule with 6.2 Å (= 0.62 nm) as its second largest dimension (TCE 6.6 Å × 6.2 Å × 3.6 Å; Karanfil and Dastgheib 2004), compared to PCE with 6.6 Å (= 0.66 nm) (Bembnowska et al. 2003). Both compounds can be subject to size exclusion when the pore width of the sorbent becomes smaller than 1.7 times of their second largest dimension (Kasaoka et al. 1989, as cited in Li et al. 2002). The shift towards larger pores in leached BC-WC dampens this size exclusion of PCE, which is also reflected by a larger increase of V_0 after leaching (TCE 7.5%; PCE 27%). Consequently, the differences between V_0 of both compounds also decreased (orig. 48%; leach. 34%) and sorption of PCE to leached BC-WC is now entirely taking place via pore-filling.

BC-GH experienced less obvious changes after the leaching procedure. The increase of pores around 1.2 nm width goes along with diminished pore volume between 0.8 and 1 nm. The diameter determining size exclusion of TCE and PCE is about 1.05 nm and 1.12 nm, respectively. Therefore, the decrease in pores smaller than 1 nm should not negatively influence sorption. Instead, V_0 of TCE increases because the larger pores in the leached sample are easier to access for the molecule. PCE, however, seems to still experience size exclusion from some pores, due to its bigger size. Therefore, V_0 of PCE only increases slightly and the change is not statistically significant.

Although PV_{tot} (= PV_{mes}) of BC-CM increases substantially after leaching (about 2-fold) and the pore size distribution experiences great changes, the effect on V_0 for both compounds is relatively small. As previously described ("Change of biochar surface and pore structure after leaching" section), leaching of BC-CM mainly opens pores in the region

Table 4 Isotherm parameters of the combined partitioning and pore-filling model for sorption of trichloroethylene (TCE) and tetrachloroethylene (PCE) to the original and leached biochars (BCs)

			K_p (L kg^{-1}) [b]	V_0 (cm^3 kg^{-1}) [b]	E (J mol^{-1}) [b]	r^2 (–) [c]	p (–) [c]
TCE	BC-WC	Original [a]	n.a.[d]	85 ± 1.3	14,452 ± 193	0.96	< 0.01
		Leached	n.a.[d]	92 ± 1.0	14,849 ± 137	0.99	< 0.01
	BC-GH	Original [a]	96 ± 35	44 ± 2.4	13,734 ± 361	0.99	< 0.01
		Leached	n.a.[d]	52 ± 0.7	13,564 ± 152	0.99	< 0.01
	BC-CM	Original [a]	50 ± 4	6 ± 0.3	14,078 ± 355	0.99	< 0.01
		Leached	61 ± 7	7 ± 0.5	13,033 ± 403	0.99	< 0.01
PCE	BC-WC	Original [a]	218 ± 51	44 ± 2.2	10,088 ± 350	0.97	< 0.01
		Leached	156 ± 51	60 ± 2.4	10,135 ± 284	0.99	< 0.01
	BC-GH	Original [a]	132 ± 39	30 ± 1.5	10,266 ± 318	0.97	< 0.01
		Leached	214 ± 37	34 ± 1.4	10,608 ± 288	0.99	< 0.01
	BC-CM	Original [a]	73 ± 6	3 ± 0.3	10,278 ± 525	0.99	< 0.01
		Leached	95 ± 7	4 ± 0.4	9831 ± 755	0.99	< 0.01

[a] Data obtained from Schreiter et al. (2018)

[b] Coefficients of the combined adsorption-partitioning model (± standard error) calculated using non-linear curve fitting in Sigma plot after Eq. 2

[c] r^2 and p represent the coefficient of determination and significance of the data fit obtained from Sigma Plot

[d] Derived K_p values were not significant ($p > 0.01$)

between 2 and 10 nm. These appear to provide additional sorption sites, resulting in the increase of V_0 of TCE after leaching. However, the larger mesopores in BC-CM are likely less favorable for contaminant sorption, compared to the narrow micropores present in the two plant-based BCs (Lastoskie et al. 1993). Therefore, the more hydrophobic molecule PCE is not highly attracted to these new sorption sites and instead favors the available partitioning domains.

The linear partitioning coefficient K_p generally experiences less obvious changes, probably because of significantly lower contribution of partitioning to the overall sorption (Table S7). Only the K_p value of PCE sorption to BC-CM significantly increases after leaching ($K_p^{PCE}{}_{leach.} > K_p^{PCE}{}_{orig.}$; $p < 0.05$). However, also K_p for TCE sorption to BC-CM tends to increase, although the change is not significant ($p > 0.05$). These changes are consistent with the observed increasing n values determined by the Freundlich model. Both indicate enhanced partitioning into the manure-derived BC after leaching. We previously reported that increasing polarity favors partitioning (Schreiter et al. 2018), because it increases the water clustering on the surface (Li et al. 2002) and might hinder the access to pores. However, it appears that the loss of oxygen-bearing functional groups (decreasing (O + N)/C) in BC-CM through leaching enhances partitioning. This indicates that the effect of pore blocking by water clusters might not be dominating in the mesoporous BC-CM. Instead, the decreasing number of functional groups increases the overall hydrophobicity (decreasing O/C), making the BC matrix more attractive for partitioning of hydrophobic molecules, such as TCE and PCE. Luo et al. (2017) also concluded that oxygen-rich leachable OC can cover aromatic structures on BC surfaces, which might hinder the partitioning of organic contaminants. This confirms that the high amount of leached DOC is responsible for the increasing K_p values of leached BC-CM by exposing additional partitioning domains. It reflects also in the increased overall percentage of partitioning, especially for the more hydrophobic compound PCE (At 5% of S_W: $PCE_{orig.}$ 13%, $PCE_{leach.}$ 16%; Table S7). For both plant-based BCs, no significant changes are evident for K_p and generally the role of partitioning in sorption decreases (Table S7). This is the case because no significant change in O/C and (O + N)/C occurred for these BCs, and consequently, both compounds are attracted to the newly accessible micropores in the leached samples.

Conclusion

The present study illustrates that accelerated leaching of BCs can significantly impact their properties and sorption behavior for chlorinated hydrocarbons. BCs produced from different feedstocks show unique changes in their structure, which results in distinct changes in sorption mechanisms. In the plant-based BCs, leaching of small amounts of ions and DOC exposed additional micropores and notably changed their size distribution. This increases the accessibility of sorption sites in small micropores and enhanced pore-filling of TCE and PCE. In contrast, the release of high ion and DOC concentrations from the manure-based BC only modified external surface area and mesopore volume, which showed little effect on sorption. Instead, the removal of oxygen-containing functional groups, and resulting increasing hydrophobicity and lower

polarity, enhanced the accessibility of partitioning domains and therefore increased its contribution to overall sorption.

This highlights that both leachable OC and minerals can play an important role in modifying the chemical and structural characteristics of BC and thus influence organic contaminant sorption. Thereby, the impact on sorption is not mainly driven by the mass leached, but rather by the release mechanism and spatial distribution of leachable constituents. Considering BC application in environmental remediation, the results imply that leaching can significantly alter the environmental fate of organic contaminants in BC-amended soils over time. Sorption is not constant and tends to increase with DOC and mineral release during "aging", making BC a potential long-term sink for hydrophobic organic contaminants.

Acknowledgements We kindly thank three anonymous reviewers whose comments helped to improve this manuscript.

Funding information The authors received financial support from the German-Israeli Foundation for Scientific Research and Development (Grant Number: G-1263-307.8/2014).

Compliance with ethical standards

Conflict of interest The authors declare that they have no conflict of interest.

References

Allen-King RM, Grathwohl P, Ball WP (2002) New modeling paradigms for the sorption of hydrophobic organic chemicals to heterogeneous carbonaceous matter in soils, sediments, and rocks. Adv Water Resour 25:985–1016. https://doi.org/10.1016/S0309-1708(02)00045-3

Angst TE, Sohi SP (2013) Establishing release dynamics for plant nutrients from biochar. GCB Bioenergy 5:221–226. https://doi.org/10.1111/gcbb.12023

ASTM D 1762-84 (2013) Standard test method for chemical analysis of wood charcoal. ASTM International, West Conshohocken, PA

Bembnowska A, Pełech R, Milchert E (2003) Adsorption from aqueous solutions of chlorinated organic compounds onto activated carbons. J Colloid Interface Sci 265:276–282. https://doi.org/10.1016/S0021-9797(03)00532-0

Cao X, Harris W (2010) Properties of dairy-manure-derived biochar pertinent to its potential use in remediation. Bioresour Technol 101:5222–5228. https://doi.org/10.1016/j.biortech.2010.02.052

Carmo AM, Hundal LS, Thompson ML (2000) Sorption of hydrophobic organic compounds by soil materials: application of unit equivalent Freundlich coefficients. Environ Sci Technol 34:4363–4369. https://doi.org/10.1021/es000968v

Chen B, Zhou D, Zhu L (2008) Transitional adsorption and partition of nonpolar and polar aromatic contaminants by biochars of pine needles with different pyrolytic temperatures. Environ Sci Technol 42:5137–5143. https://doi.org/10.1021/es8002684

Christophe N, Cyril G, Romain L, Alessandro P, Robert M, Arne S, Cornelia R (2015) Effect of physical weathering on the carbon sequestration potential of biochars and hydrochars in soil. GCB Bioenergy 7:488–496. https://doi.org/10.1111/gcbb.12158

Chun Y, Sheng G, Chiou CT, Xing B (2004) Compositions and sorptive properties of crop residue-derived chars. Environ Sci Technol 38:4649–4655. https://doi.org/10.1021/es035034w

Cumming G (2009) Inference by eye: reading the overlap of independent confidence intervals. Stat Med 28:205–220. https://doi.org/10.1002/sim.3471

de Figueredo NA, da Costa LM, Melo LCA, Siebeneichlerd EA, Tronto J (2017) Characterization of biochars from different sources and evaluation of release of nutrients and contaminants. Rev Ciênc Agron 48:395–403. https://doi.org/10.5935/1806-6690.20170046

Feng M, Zhang W, Wu X, Jia Y, Jiang C, Wei H, Qiu R, Tsang DCW (2018) Continuous leaching modifies the surface properties and metal(loid) sorption of sludge-derived biochar. Sci Total Environ 625:731–737. https://doi.org/10.1016/j.scitotenv.2017.12.337

Fu H, Wei C, Qu X, Li H, Zhu D (2018) Strong binding of apolar hydrophobic organic contaminants by dissolved black carbon released from biochar: a mechanism of pseudomicelle partition and environmental implications. Environ Pollut 232:402–410. https://doi.org/10.1016/j.envpol.2017.09.053

Graber ER, Meller Harel Y, Kolton M, Cytryn E, Silber A, Rav David D, Tsechansky L, Borenshtein M, Elad Y (2010) Biochar impact on development and productivity of pepper and tomato grown in fertigated soilless media. Plant Soil 337:481–496. https://doi.org/10.1007/s11104-010-0544-6

Gul S, Whalen JK, Thomas BW, Sachdeva V, Deng H (2015) Physico-chemical properties and microbial responses in biochar-amended soils: mechanisms and future directions. Agric Ecosyst Environ 206:46–59. https://doi.org/10.1016/j.agee.2015.03.015

Hollister CC, Bisogni JJ, Lehmann J (2013) Ammonium, nitrate, and phosphate sorption to and solute leaching from biochars prepared from corn stover (Zea mays L.) and Oak Wood (Quercus spp.). J Environ Qual 42:137–144. https://doi.org/10.2134/jeq2012.0033

Jamieson T, Sager E, Guéguen C (2014) Characterization of biochar-derived dissolved organic matter using UV–visible absorption and excitation–emission fluorescence spectroscopies. Chemosphere 103:197–204. https://doi.org/10.1016/j.chemosphere.2013.11.066

Kah M, Sun H, Sigmund G, Hüffer T, Hofmann T (2016) Pyrolysis of waste materials: characterization and prediction of sorption potential across a wide range of mineral contents and pyrolysis temperatures. Bioresour Technol 214:225–233. https://doi.org/10.1016/j.biortech.2016.04.091

Karanfil T, Dastgheib SA (2004) Trichloroethylene adsorption by fibrous and granular activated carbons: aqueous phase, gas phase, and water vapor adsorption studies. Environ Sci Technol 38:5834–5841. https://doi.org/10.1021/es0497936

Kasaoka S, Sakata Y, Tanaka E, Naitoh R (1989) Design of molecular-sieving carbon. Studies on adsorption of various dyes in liquid phase. Int Chem Eng 29:734–742. https://doi.org/10.1246/nikkashi.1987.2260

Klasson KT, Uchimiya M, Lima IM (2014) Uncovering surface area and micropores in almond shell biochars by rainwater wash. Chemosphere 111:129–134. https://doi.org/10.1016/j.chemosphere.2014.03.065

Kleineidam S, Schüth C, Grathwohl P (2002) Solubility-normalized combined adsorption-partitioning sorption isotherms for organic pollutants. Environ Sci Technol 36:4689–4697. https://doi.org/10.1021/es010293b

Kloss S, Zehetner F, Dellantonio A, Hamid R, Ottner F, Liedtke V, Schwanninger M, Gerzabek MH, Soja G (2012) Characterization of slow pyrolysis biochars: effects of feedstocks and pyrolysis temperature on biochar properties. J Environ Qual 41:990–1000. https://doi.org/10.2134/jeq2011.0070

Kong Z, Liaw SB, Gao X, Yu Y, Wu H (2014) Leaching characteristics of inherent inorganic nutrients in biochars from the slow and fast pyrolysis of mallee biomass. Fuel 128:433–441. https://doi.org/10.1016/j.fuel.2014.03.025

Kumar A, Schreiter IJ, Wefer-Roehl A, Tsechansky L, Schüth C, Graber ER (2016) Production and utilization of biochar from organic wastes for pollutant control on contaminated sites. In: Prasad MNV, Shih K (eds) Environmental materials and waste. Academic Press, Cambridge, pp 91–116

Kumar A, Elad Y, Tsechansky L, Abrol V, Lew B, Offenbach R, Graber ER (2018) Biochar potential in intensive cultivation of Capsicum annuum L. (sweet pepper): crop yield and plant protection. J Sci Food Agric 98:495–503. https://doi.org/10.1002/jsfa.8486

Kwon S, Pignatello JJ (2005) Effect of natural organic substances on the surface and adsorptive properties of environmental black carbon (char): pseudo pore blockage by model lipid components and its implications for N2-probed surface properties of natural sorbents. Environ Sci Technol 39:7932–7939. https://doi.org/10.1021/es050976h

Lastoskie C, Gubbins KE, Quirke N (1993) Pore size distribution analysis of microporous carbons: a density functional theory approach. J Phys Chem 97:4786–4796. https://doi.org/10.1021/j100120a035

Lehmann J, Joseph S (2009) Biochar for environmental management: an introduction. In: Lehmann J, Joseph S (eds) Biochar for environmental management: science and technology. Earthscan, London, p 416

Leite AB, Saucier C, Lima EC, dos Reis GS, Umpierres CS, Mello BL, Shirmardi M, Dias SLP, Sampaio CH (2018) Activated carbons from avocado seed: optimisation and application for removal of several emerging organic compounds. Environ Sci Pollut Res 25:7647–7661. https://doi.org/10.1007/s11356-017-1105-9

Li L, Quinlivan PA, Knappe DRU (2002) Effects of activated carbon surface chemistry and pore structure on the adsorption of organic contaminants from aqueous solution. Carbon 40:2085–2100. https://doi.org/10.1016/S0008-6223(02)00069-6

Lin Y, Munroe P, Joseph S, Henderson R, Ziolkowski A (2012a) Water extractable organic carbon in untreated and chemical treated biochars. Chemosphere 87:151–157. https://doi.org/10.1016/j.chemosphere.2011.12.007

Lin Y, Munroe P, Joseph S, Kimber S, Van Zwieten L (2012b) Nanoscale organo-mineral reactions of biochars in ferrosol: an investigation using microscopy. Plant Soil 357:369–380. https://doi.org/10.1007/s11104-012-1169-8

Liu G, Zheng H, Jiang Z, Zhao J, Wang Z, Pan B, Xing B (2018) Formation and physicochemical characteristics of nano biochar: insight into chemical and colloidal stability. Environ Sci Technol 52:10369–10379. https://doi.org/10.1021/acs.est.8b01481

Liu C-H, Chu W, Li H, Boyd SA, Teppen BJ, Mao J, Lehmann J, Zhang W (2019) Quantification and characterization of dissolved organic carbon from biochars. Geoderma 335:161–169. https://doi.org/10.1016/j.geoderma.2018.08.019

Luo L, Lv J, Chen Z, Huang R, Zhang S (2017) Insights into the attenuated sorption of organic compounds on black carbon aged in soil. Environ Pollut 231:1469–1476. https://doi.org/10.1016/j.envpol.2017.09.010

Nguyen TH, Cho H-H, Poster DL, Ball WP (2007) Evidence for a pore-filling mechanism in the adsorption of aromatic hydrocarbons to a natural wood char. Environ Sci Technol 41:1212–1217. https://doi.org/10.1021/es0617845

Norwood MJ, Louchouarn P, Kuo L-J, Harvey OR (2013) Characterization and biodegradation of water-soluble biomarkers and organic carbon extracted from low temperature chars. Org Geochem 56:111–119. https://doi.org/10.1016/j.orggeochem.2012.12.008

Qu X, Fu H, Mao J, Ran Y, Zhang D, Zhu D (2016) Chemical and structural properties of dissolved black carbon released from biochars. Carbon 96:759–767. https://doi.org/10.1016/j.carbon.2015.09.106

Ren X, Sun H, Wang F, Zhang P, Zhu H (2018) Effect of aging in field soil on biochar's properties and its sorption capacity. Environ Pollut. https://doi.org/10.1016/j.envpol.2018.07.078

Schreiter IJ, Schmidt W, Schüth C (2018) Sorption mechanisms of chlorinated hydrocarbons on biochar produced from different feedstocks: conclusions from single- and bi-solute experiments. Chemosphere 203:34–43. https://doi.org/10.1016/j.chemosphere.2018.03.173

Smith CR, Sleighter RL, Hatcher PG, Lee JW (2013) Molecular characterization of inhibiting biochar water-extractable substances using electrospray ionization fourier transform ion cyclotron resonance mass spectrometry. Environ Sci Technol 47:13294–13302. https://doi.org/10.1021/es4034777

Smith CR, Hatcher PG, Kumar S, Lee JW (2016) Investigation into the sources of biochar water-soluble organic compounds and their potential toxicity on aquatic microorganisms. ACS Sustain Chem Eng 4:2550–2558. https://doi.org/10.1021/acssuschemeng.5b01687

Spokas KA, Novak JM, Masiello CA, Johnson MG, Colosky EC, Ippolito JA, Trigo C (2014) Physical disintegration of biochar: an overlooked process. Environ Sci Technol Lett 1:326–332. https://doi.org/10.1021/ez500199t

Tang J, Li X, Luo Y, Li G, Khan S (2016) Spectroscopic characterization of dissolved organic matter derived from different biochars and their polycylic aromatic hydrocarbons (PAHs) binding affinity. Chemosphere 152:399–406. https://doi.org/10.1016/j.chemosphere.2016.03.016

Trigo C, Spokas KA, Cox L, Koskinen WC (2014) Influence of soil biochar aging on sorption of the herbicides MCPA, nicosulfuron, terbuthylazine, indaziflam, and fluoroethyldiaminotriazine. J Agric Food Chem 62:10855–10860. https://doi.org/10.1021/jf5034398

Wang B, Zhang W, Li H, Fu H, Qu X, Zhu D (2017) Micropore clogging by leachable pyrogenic organic carbon: a new perspective on sorption irreversibility and kinetics of hydrophobic organic contaminants to black carbon. Environ Pollut 220:1349–1358. https://doi.org/10.1016/j.envpol.2016.10.100

Wu H, Yip K, Kong Z, Li C-Z, Liu D, Yu Y, Gao X (2011) Removal and recycling of inherent inorganic nutrient species in mallee biomass and derived biochars by water leaching. Ind Eng Chem Res 50:12143–12151. https://doi.org/10.1021/ie200679n

Wu H, Che X, Ding Z, Hu X, Creamer AE, Chen H, Gao B (2016) Release of soluble elements from biochars derived from various biomass feedstocks. Environ Sci Pollut Res 23:1905–1915. https://doi.org/10.1007/s11356-015-5451-1

Xia G, Ball WP (1999) Adsorption-partitioning uptake of nine low-polarity organic chemicals on a natural sorbent. Environ Sci Technol 33:262–269. https://doi.org/10.1021/es980581g

Xiao X, Chen B, Chen Z, Zhu L, Schnoor JL (2018) Insight into multiple and multilevel structures of biochars and their potential environmental applications: a critical review. Environ Sci Technol 52:5027–5047. https://doi.org/10.1021/acs.est.7b06487

Xu X, Zhao Y, Sima J, Zhao L, Mašek O, Cao X (2017) Indispensable role of biochar-inherent mineral constituents in its environmental applications: a review. Bioresour Technol 241:887–899. https://doi.org/10.1016/j.biortech.2017.06.023

Yang H, Yan R, Chen H, Lee DH, Zheng C (2007) Characteristics of hemicellulose, cellulose and lignin pyrolysis. Fuel 86:1781–1788. https://doi.org/10.1016/j.fuel.2006.12.013

Yang Y, Sun K, Han L, Jin J, Sun H, Yang Y, Xing B (2018) Effect of minerals on the stability of biochar. Chemosphere 204:310–317. https://doi.org/10.1016/j.chemosphere.2018.04.057

Yao FX, Arbestain MC, Virgel S, Blanco F, Arostegui J, Maciá-Agulló JA, Macías F (2010) Simulated geochemical weathering of a mineral ash-rich biochar in a modified Soxhlet reactor. Chemosphere 80:724–732. https://doi.org/10.1016/j.chemosphere.2010.05.026

Zama EF, Reid BJ, Arp HPH, Sun G-X, Yuan H-Y, Zhu Y-G (2018) Advances in research on the use of biochar in soil for remediation:

a review. J Soils Sediments 18:2433–2450. https://doi.org/10.1007/s11368-018-2000-9

Zhang X, Wang H, He L, Lu K, Sarmah A, Li J, Bolan N, Pei J, Huang H (2013) Using biochar for remediation of soils contaminated with heavy metals and organic pollutants. Environ Sci Pollut Res 20:8472–8483. https://doi.org/10.1007/s11356-013-1659-0

Zhang C, Liu L, Zhao M, Rong H, Xu Y (2018) The environmental characteristics and applications of biochar. Environ Sci Pollut Res 25:21525–21534. https://doi.org/10.1007/s11356-018-2521-1

Zhao L, Cao X, Wang Q, Yang F, Xu S (2013) Mineral constituents profile of biochar derived from diversified waste biomasses: implications for agricultural applications. J Environ Qual 42:545–552. https://doi.org/10.2134/jeq2012.0232